Supplementary Information (SI) for Dalton Transactions.

Substituent Effect on the Boron Atoms in Boron-Bridged Hexazenes

Masahiro Yamamoto, and Makoto Yamashita*

Table of Contents

1. Experimental Procedures

General

All manipulations involving the air- and moisture-sensitive compounds were carried out under an argon atmosphere using standard Schlenk and glovebox (Korea KIYON, Korea and ALS Technology, Japan) technique. Dry dichloromethane, Et_2O, and hexane were purified by passing through a solvent purification system (Glass Contour). **1** was synthesized by using the procedures reported in the literature.[30] $CDCl_3$ (Kanto), trifluoromethanesulfonic acid (TCI), tetrabutylammonium chloride (TCI), and methylmagnesium bromide (Sigma-Aldrich) were purchased and used as received. The nuclear magnetic resonance (NMR) spectra were recorded on a JEOL ECS-400 [399 MHz for ^1H, 128 MHz for $^{11}B\{^1H\}$, 100 MHz for $^{13}C\{^1H\}$] spectrometers. Melting points were determined on the Optimelt (SRS) without compensation. Elemental analyses were performed on a Perkin-Elmer 2400 series II CHN analyzer. UV-vis absorption spectra were recorded on a Shimadzu UV-3600 spectrometer. Emission spectra were recorded on a JASCO FP-8200 spectrometer, and absolute fluorescence quantum yields were measured by the photon-counting method using an integration sphere on a JASCO FP-6500 or HAMAMATSU Quantaurus-QY spectrometer. Electrochemical measurements were performed using an ALS 600D potentiostat/galvanostat.

Synthesis of 2

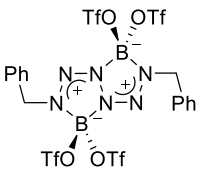

2

In a 2000 mL three-neck flask under argon atmosphere, trifluoromethanesulfonic acid (2.11 mL, 24.0 mmol) was added to a solution of **1** (3.92 g, 6.00 mmol) in dry dichloromethane (600 mL) at room temperature. After the reaction mixture was stirred at room temperature for 16 h, the reaction mixture was concentrated to ca. 20 mL under reduced pressure. The concentrated solution was added dropwise to hexane (1.0 L) in a 1 L flask under stirring. The resulting mixture was filtered through a filter paper, and the filtrate was concentrated under reduced pressure to afford a light-yellow solid of **2** (4.14 g, 4.68 mmol, 78%).

^1H NMR (399 MHz, $CDCl_3$) δ 7.46–7.39 (m, 6H, Ar-H), 7.38–7.33 (m, 4H, Ar-H), 5.25 (s, 4H, NCH_2); $^{11}B\{^1H\}$ NMR (128 MHz, $CDCl_3$) δ −2 (s); $^{13}C\{^1H\}$ NMR (100 MHz, $CDCl_3$) δ 130.30 (Ar-*C*H), 129.86 (Ar-*C*), 129.67 (Ar-*C*H), 129.44 (Ar-*C*H), 118.04 (q, *J* = 319 Hz), 57.11 (N*C*H_2); $^{19}F\{^1H\}$ NMR (376 MHz, $CDCl_3$) δ −75.79 (s), Anal. Calcd. for $C_{18}H_{14}B_2F_{12}N_6O_{12}S_4$: C, 24.45; H, 1.60; N, 9.51; Found: C,24.71; H, 1.42; N, 9.19; mp: 87–91 °C (decomp.).

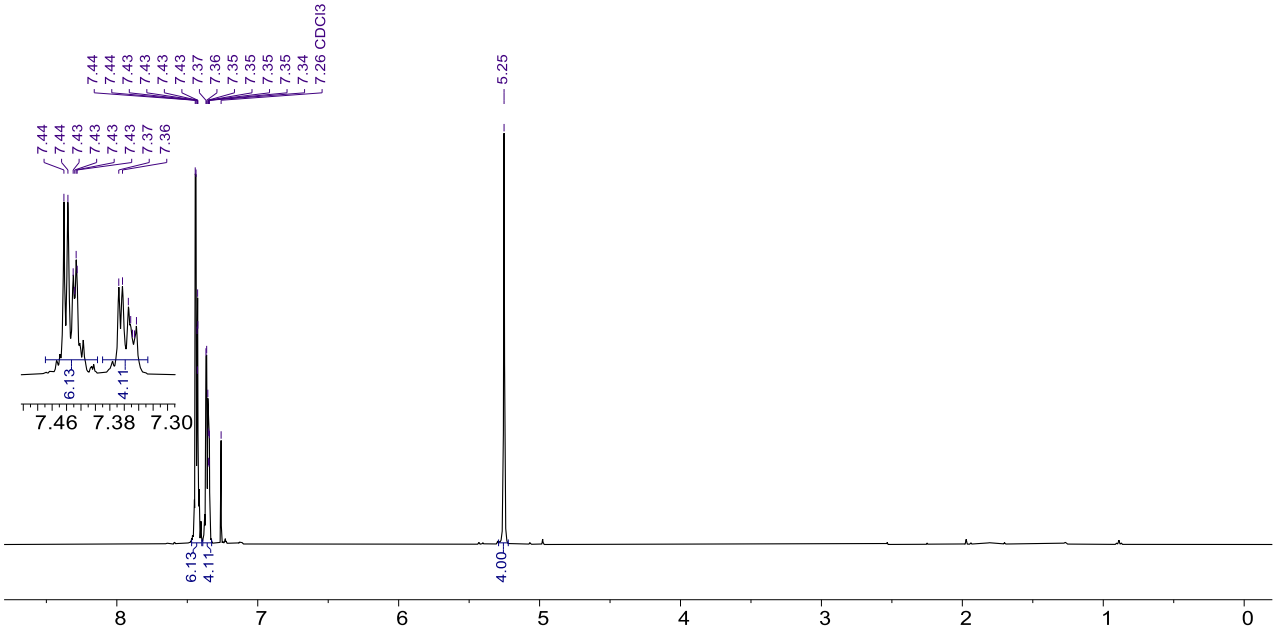

Figure S1. The ^{1}H NMR spectrum of **2** in $CDCl_3$.

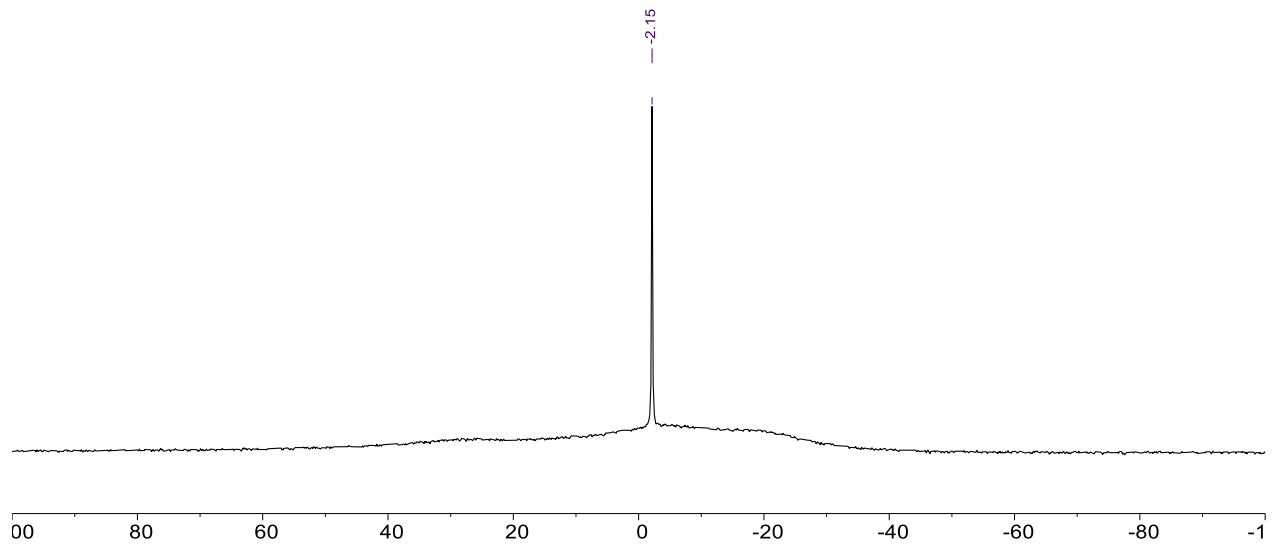

Figure S2. The $^{11}B\{^{1}H\}$ NMR spectrum of **2** in $CDCl_3$.

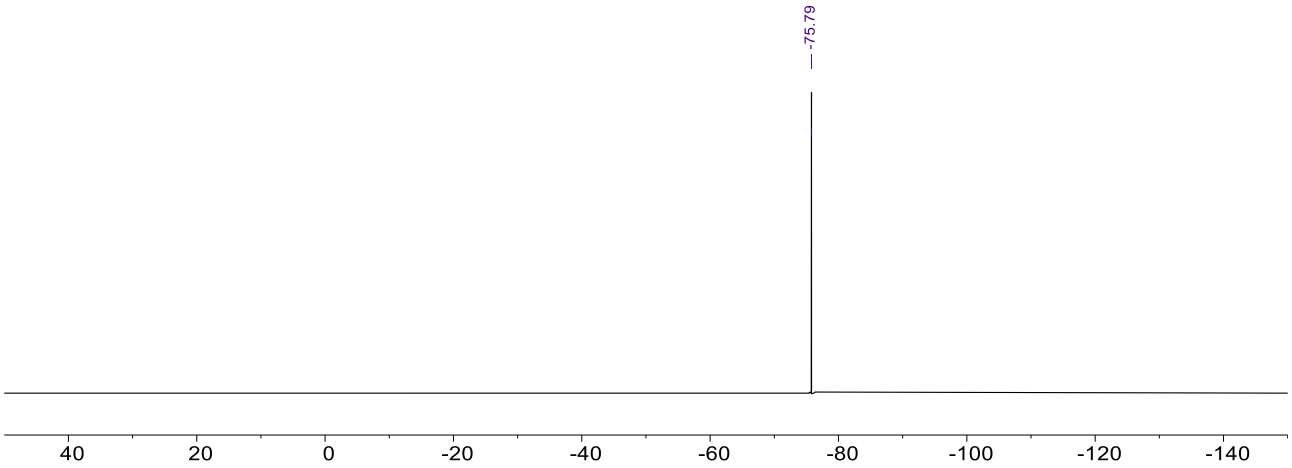

Figure S3. The $^{19}F\{^{1}H\}$ NMR spectrum of **2** in $CDCl_3$.

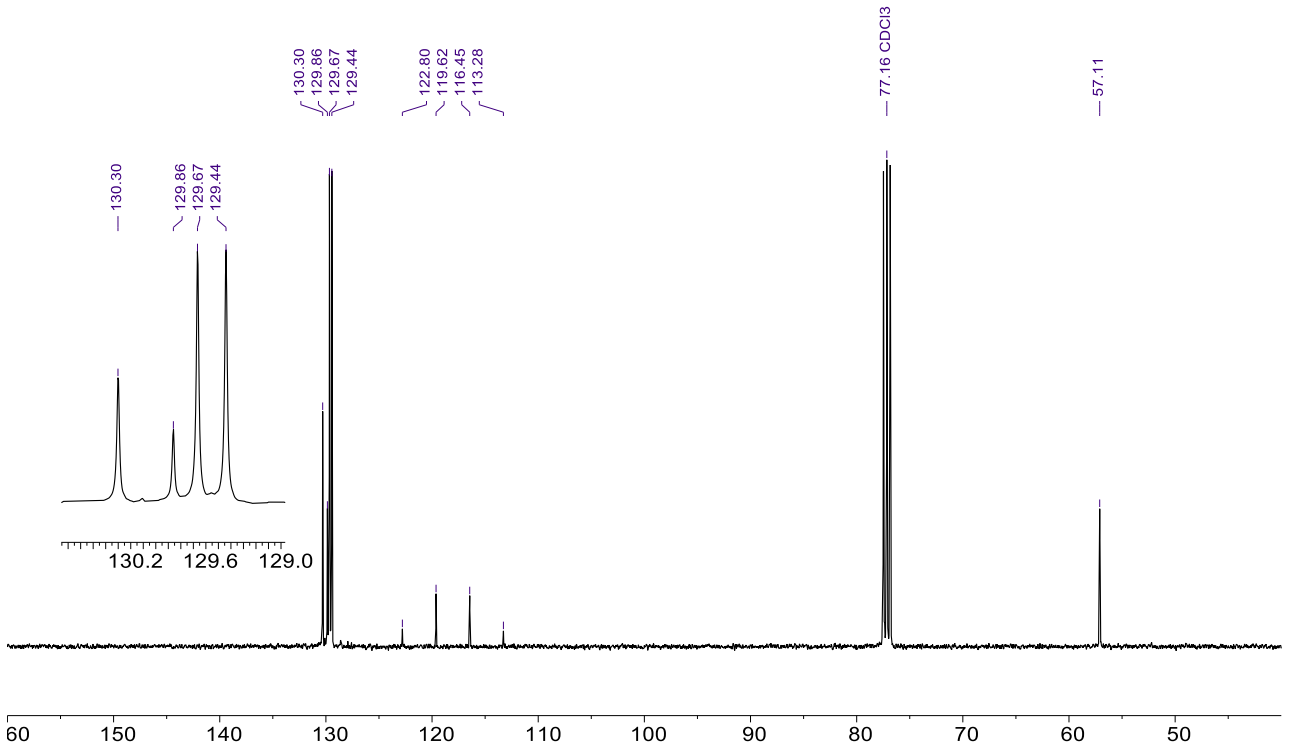

Figure S4. The $^{13}C\{^{1}H\}$ NMR spectrum of **2** in $CDCl_3$.

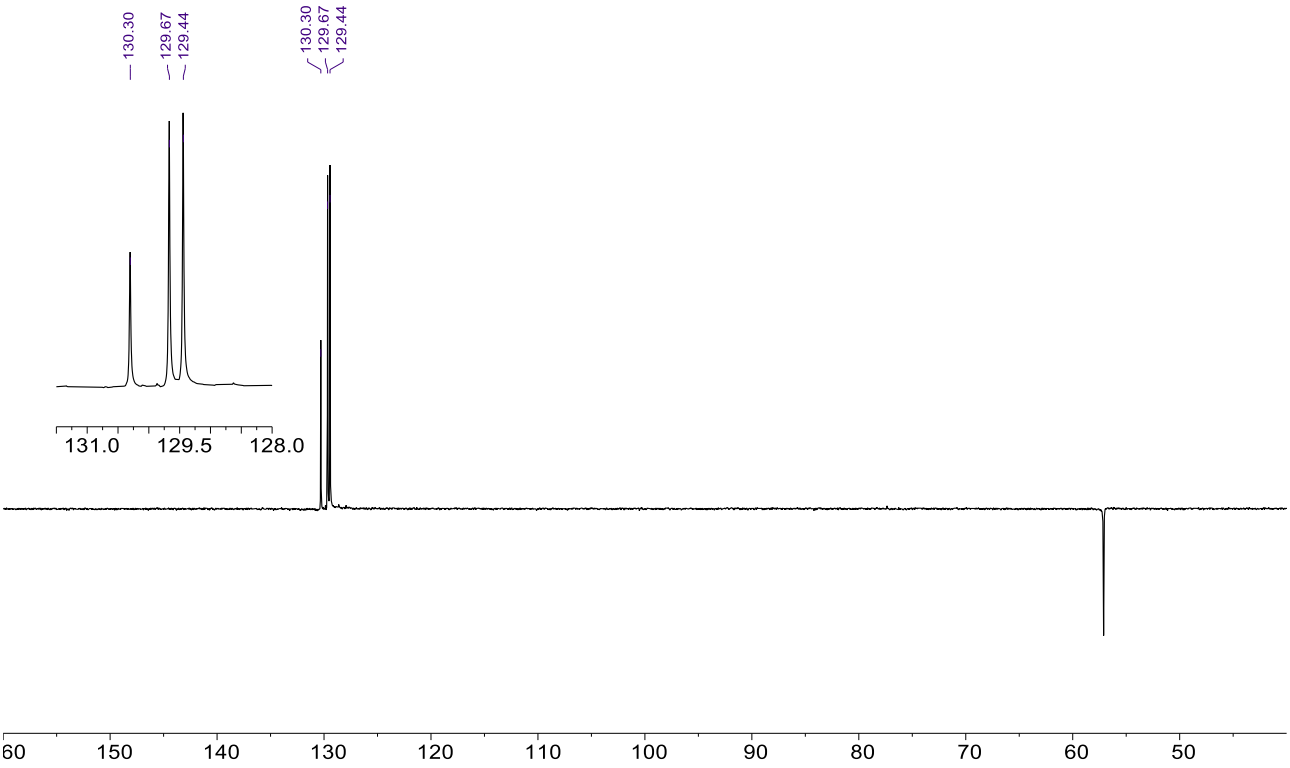

Figure S5. The $^{13}C\{^{1}H\}$ DEPT-135 NMR spectrum of **2** in $CDCl_3$.

Synthesis of 3

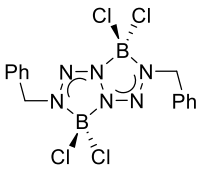

3(Cl)

In a 100 mL Schlenk flask under argon atmosphere, a solution of **2** (3.54 g, 4.00 mmol) in dry dichloromethane (10 mL) was added dropwise to a solution of tetrabutylammonium chloride (4.45 g, 16.0 mmol) in dry dichloromethane (10 mL) at room temperature. After stirring the reaction mixture for 16 h at room temperature, it was purified by passing through a short pad of silica-gel. The filtrate was concentrated under reduced pressure, and the residue was recrystallized from dichloromethane to afford light yellow crystals of **3** (1.22 g, 2.84 mmol, 71%).

^{1}H NMR (399 MHz, $CDCl_3$) δ 7.45–7.36 (m, 10H, Ar-*H*), 5.11 (s, 4H, NC*H*$_2$); ^{11}B{^{1}H} NMR (128 MHz, $CDCl_3$) δ 2 (s); ^{13}C{^{1}H} NMR (100 MHz, $CDCl_3$) δ 132.66 (Ar-*C*), 129.52 (Ar-*C*H), 129.40 (Ar-*C*H), 129.22 (Ar-*C*H), 54.78 (N*C*H$_2$); Anal. Calcd. for $C_{14}H_{14}B_2Cl_4N_6$: C, 39.13; H, 3.28; N, 19.56; Found: C, 39.19; H, 3.55; N, 19.81; mp: 169–173 °C (decomp.).

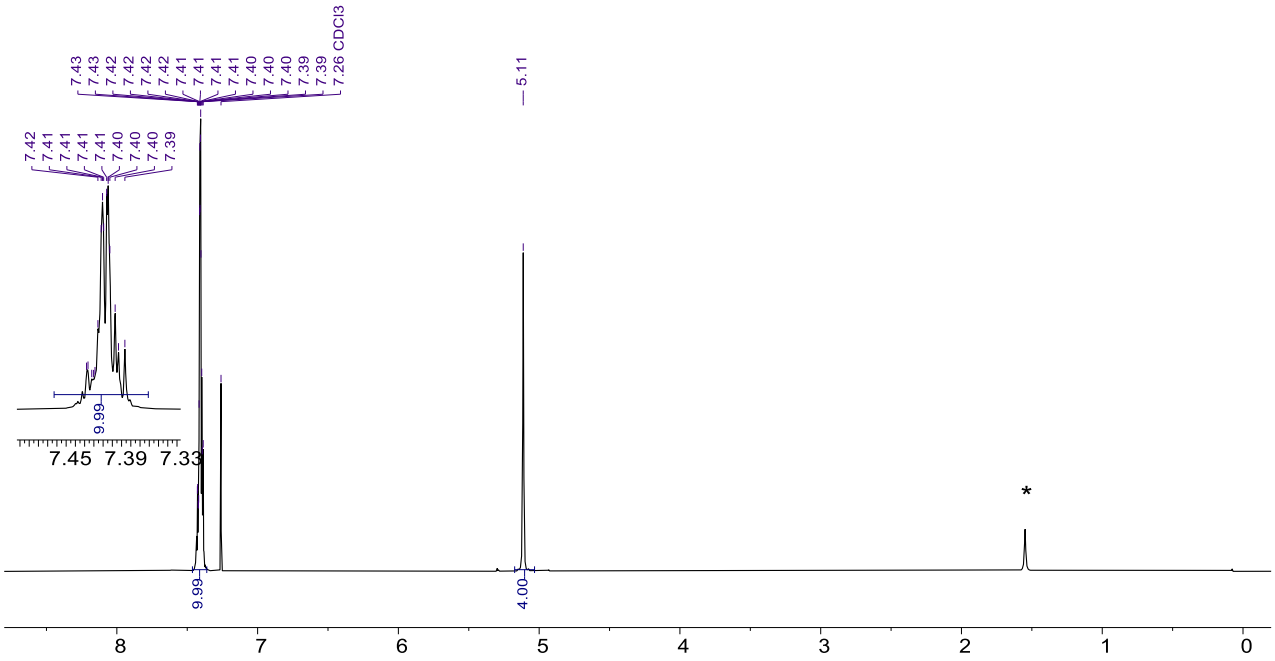

Figure S6. The ^{1}H NMR spectrum of **3** in $CDCl_3$ (*: H_2O).

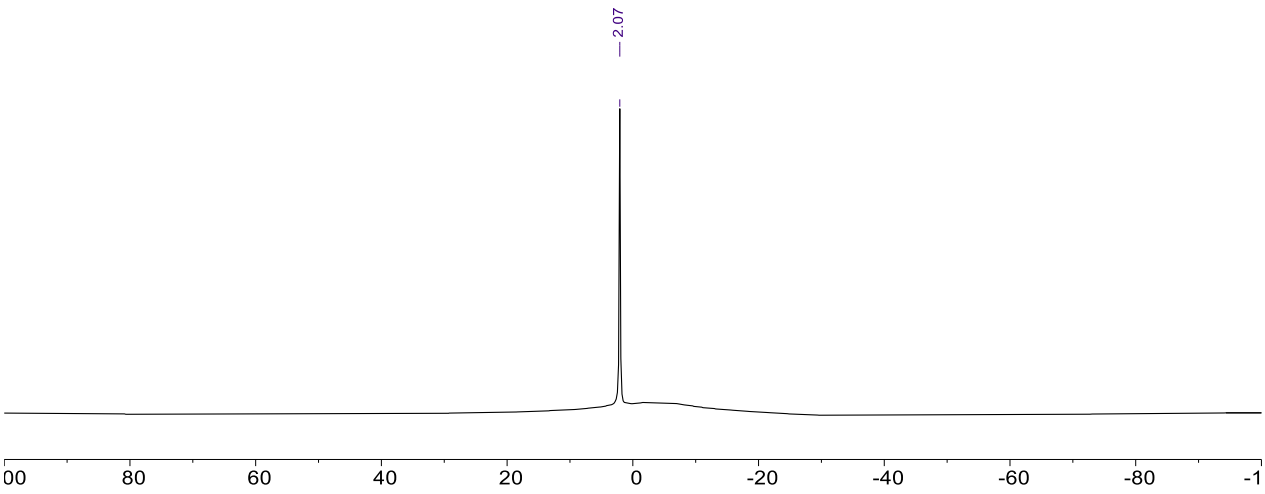

Figure S7. The ^{11}B{^{1}H} NMR spectrum of **3** in $CDCl_3$.

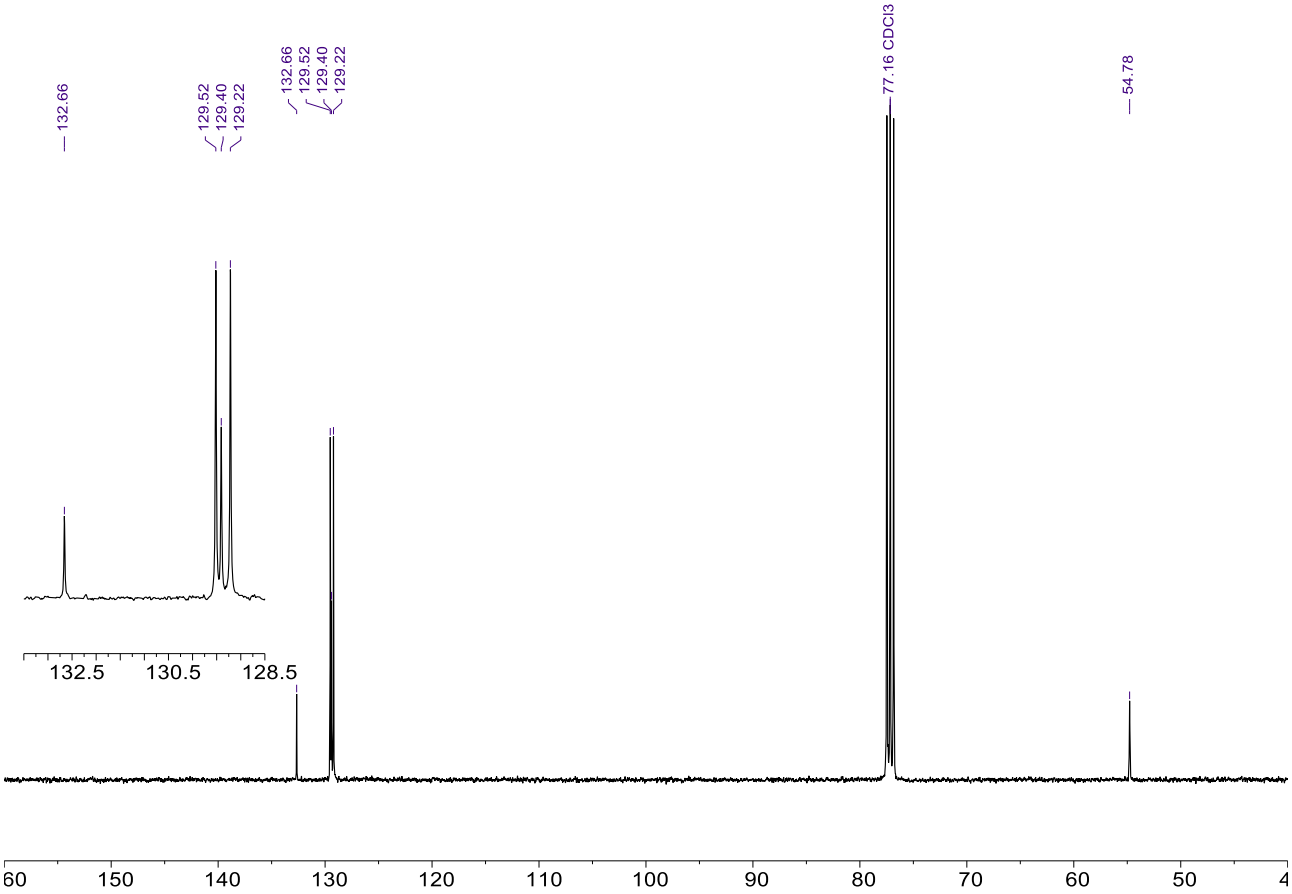

Figure S8. The $^{13}C\{^{1}H\}$ NMR spectrum of **3** in $CDCl_3$.

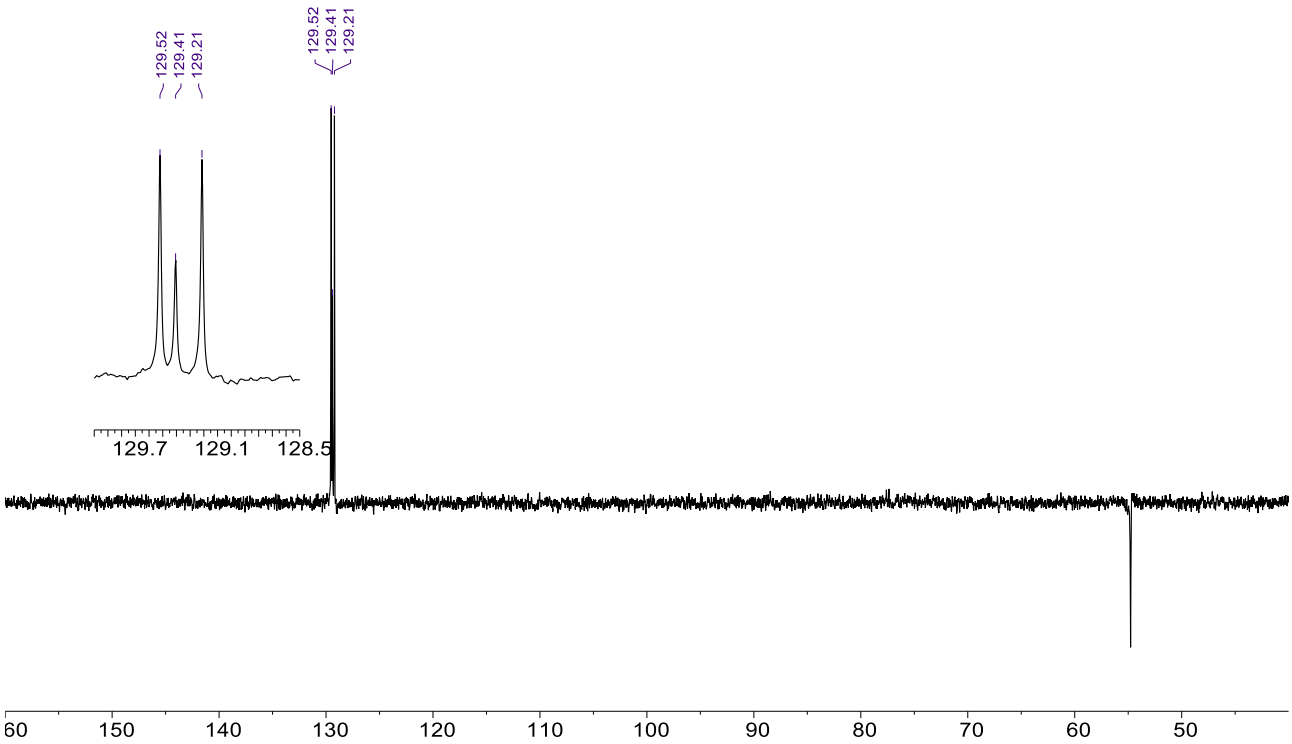

Figure S9. The $^{13}C\{^{1}H\}$ DEPT-135 NMR spectrum of **3** in $CDCl_3$.

Synthesis of 4

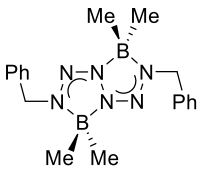

4(Me)

Method A: In a 50 mL Schlenk flask under argon atmosphere, a solution of **2** (1.77 g, 2.00 mmol) in dry hexane (20 mL) was added dropwise to a solution of $AlMe_3$ in hexane (1.4 M, 6.00 mL, 8.40 mmol) at −78°C using a dry ice/acetone bath. The mixture was then warmed to room temperature and stirred for 16 h. The reaction was quenched with water, and the mixture was extracted with hexane. The combined organic layer was dried over Na_2SO_4 and filtered through a filter paper. The filtrate was concentrated using a rotary evaporator, and the residue was recrystallized from dichloromethane to afford fluorescent yellow crystals of **4** (522 mg, 1.50 mmol, 75%).

Method B: In a 10 mL Schlenk flask under argon atmosphere, a solution of MeMgBr in diethyl ether (3.0 M, 134 µL, 401 µmol) was added dropwise to a solution of **3** (42.9 mg, 100 µmol) in dry diethyl ether (3.0 mL) at −78°C using a dry ice/acetone bath. The mixture was then warmed to room temperature and stirred for 16 h. Volatiles were removed from the reaction mixture under reduced pressure. The residue was purified by passing through a short pad of silica-gel, and the filtrate was concentrated to afford a fluorescent yellow solid of **4** (28.3 mg, 81.3 µmol, 81%).

^{1}H NMR (399 MHz, $CDCl_3$) δ 7.36–7.26 (m, 10H, Ar-*H*), 4.73 (s, 4H, NC*H*$_2$), −0.13 (s, 4H, BC*H*$_3$); ^{11}B{^{1}H} NMR (128 MHz, $CDCl_3$) δ 1 (s); ^{13}C{^{1}H} NMR (100 MHz, $CDCl_3$) δ 136.38 (Ar-*C*), 128.72 (Ar-*C*H), 128.61 (Ar-*C*H), 128.10 (Ar-*C*H), 54.26 (N*C*H$_2$), 6.94 (B*C*H$_3$); Anal. Calcd. for $C_{18}H_{26}B_2N_6$: C, 62.11; H, 7.53; N, 24.15; Found: C, 62.06; H, 7.54; N, 24.00; mp: 111–115 °C (decomp.).

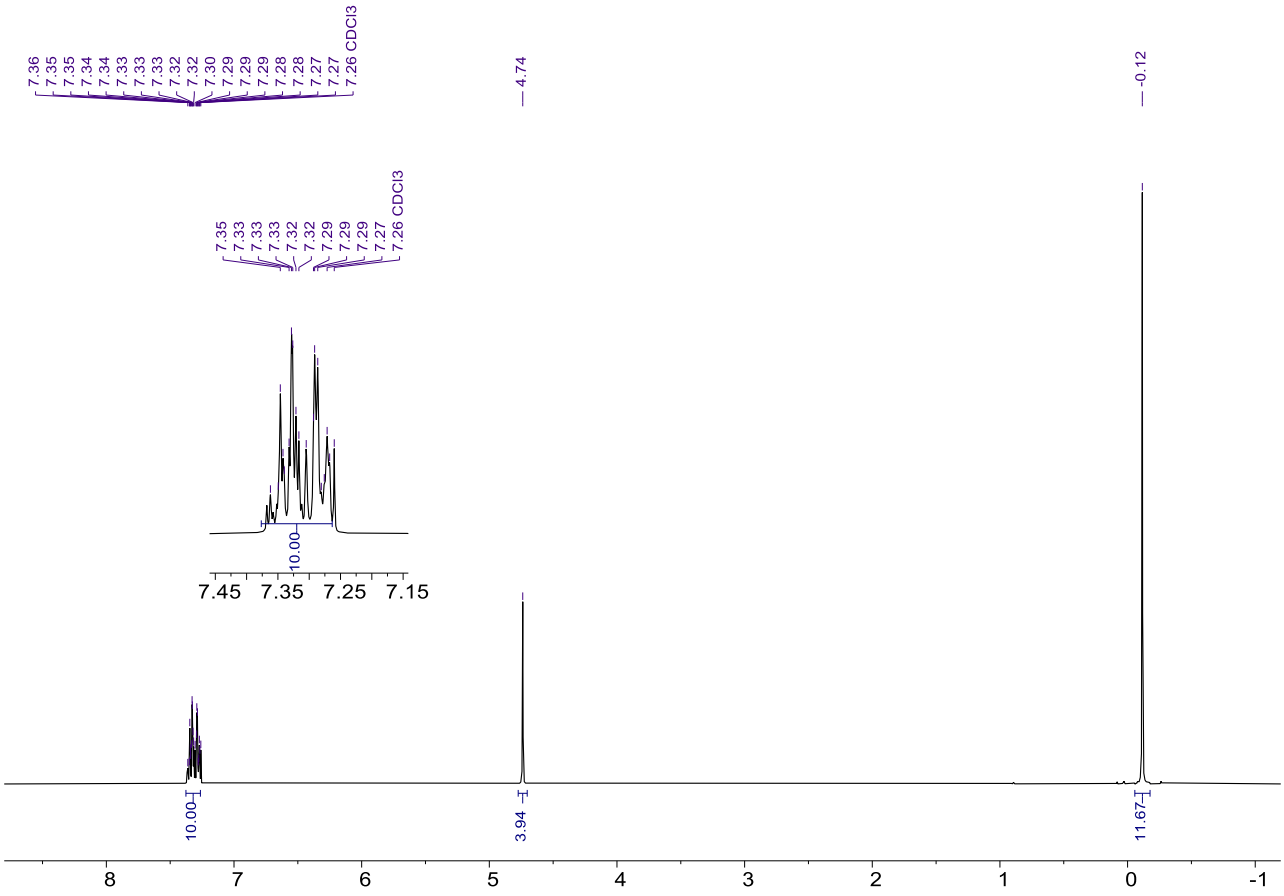

Figure S10. The ^{1}H NMR spectrum of **4** in $CDCl_3$.

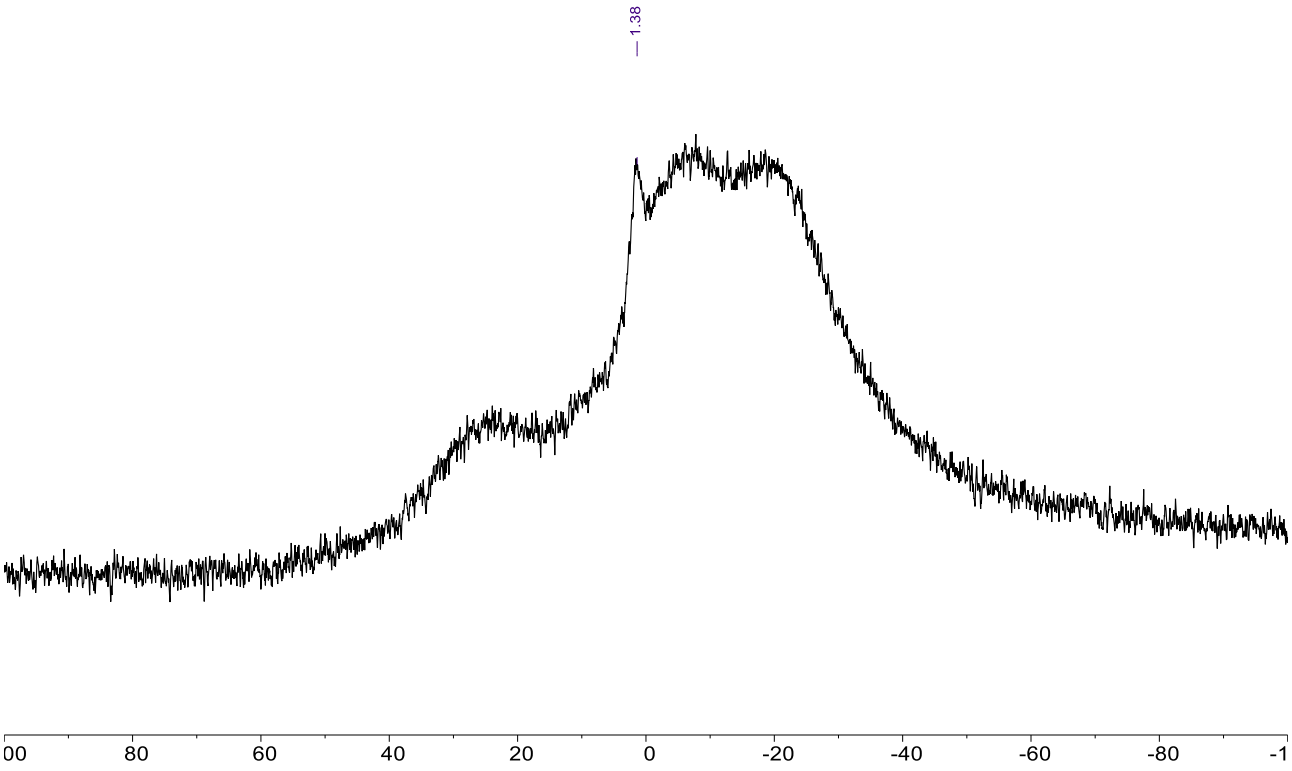

Figure S11. The $^{11}B\{^{1}H\}$ NMR spectrum of **4** in $CDCl_3$.

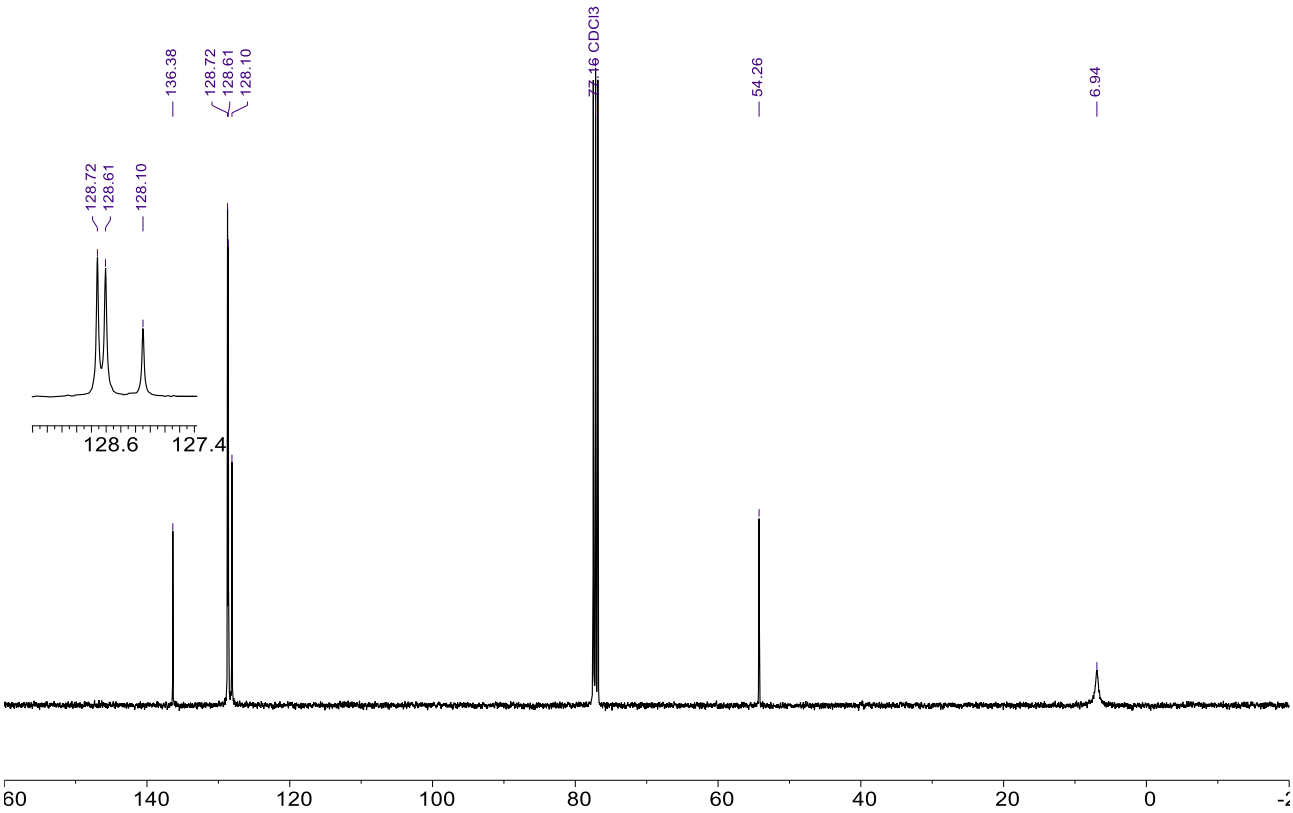

Figure S12. The $^{13}C\{^{1}H\}$ NMR spectrum of **4** in $CDCl_3$.

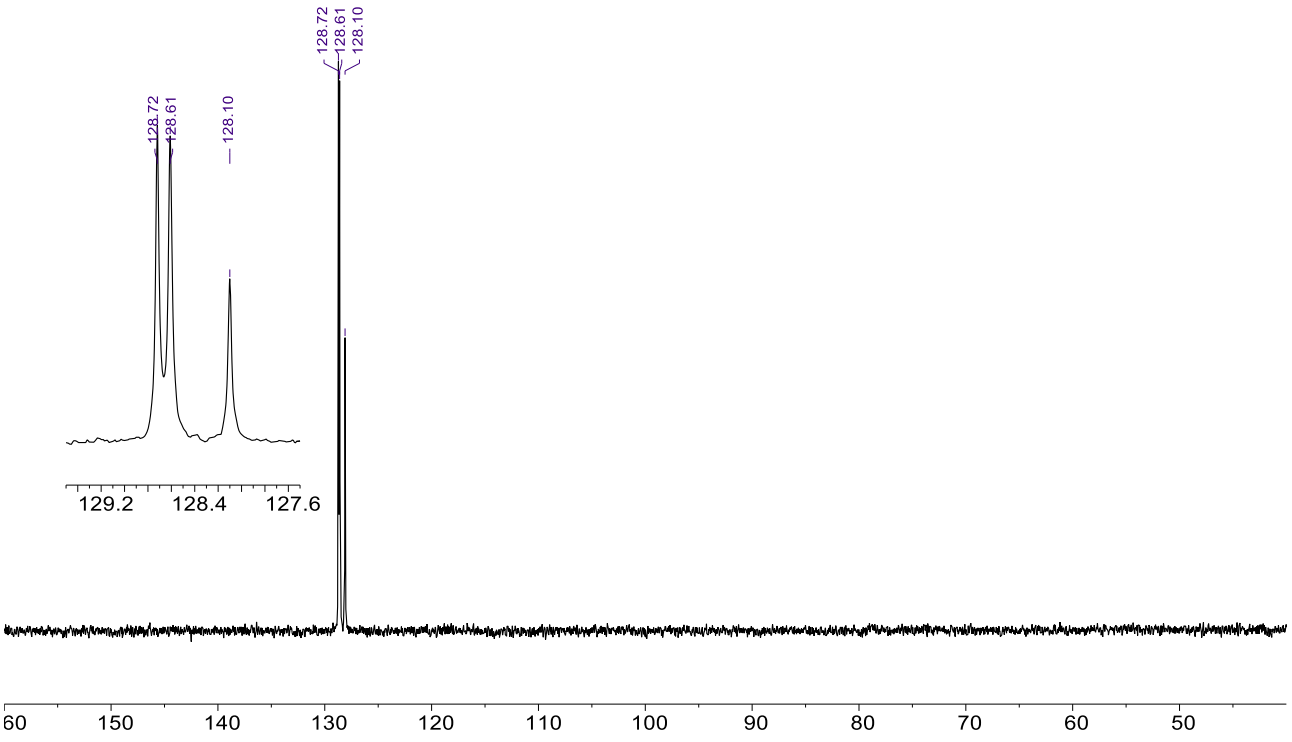

Figure S13. The $^{13}C\{^{1}H\}$ DEPT-135 NMR spectrum of **4** in $CDCl_3$.

2. Details for X-ray Crystallography

Crystallographic data for **2**, **3**, and **4** are listed in **Table S1**. The crystals were coated with immersion oil, put on a MicroMountTM (MiTeGen, LLC), and then mounted on a diffractometer. Diffraction data were collected on a Rigaku HyPix-6000 detector using MoKα radiation. The Bragg spots were integrated using the CrysAlisPro program package.[35] All the following procedures for analysis, Olex 2.0[36] and Yadokari-XG 2009[37] were used as a graphical interface. The structures were solved by direct methods using SHELXL-2018[38] and refined by full-matrix least-squares using SHELXL-2018.[38] Anisotropic temperature factors were applied to all non-hydrogen atoms. The hydrogen atoms were placed at calculated positions and refined by applying riding models. The detailed crystallographic data have been deposited with the Cambridge Crystallographic Data Centre with deposition code CCDC 2512981-2512983. A combined CIF file for the data can be obtained free of charge via http://www.ccdc.cam.ac.uk/products/csd/request.

Table S1. Crystallographic data and structure refinement details for **2**, **3**, and **4**

compound #	**2**	**3**	**4**
CCDC deposit #	2512981	2512982	2512983
Empirical formula	$C_{18}H_{14}B_2N_6O_{12}F_{12}S_4$	$C_{14}H_{14}B_2N_6Cl_4$	$C_{18}H_{26}B_2N_6$
Formula weight	884.18	429.73	348.07
T (K)	93(2)	93(2)	93(2)
λ (Å)	0.71073	0.71075	0.71075
Crystal system	*Monoclinic*	*Triclinic*	*Monoclinic*
Space group	*C2/c*	*P-1*	$P2_1/n$
a (Å)	23.1108(8)	9.510(5)	11.046(2)
b (Å)	16.0696(5)	10.265(5)	6.4077(13)
c (Å)	17.3591(6)	11.092(6)	13.815(3)
α (°)	90°	95.1397(11)	90
β (°)	92.189(3)	108.318(6)	101.687(6)
γ (°)	90°	109.543(6)	90
V (Å^3)	6442.1(4)	945.5(9)	957.5(3)
Z	8	2	2
D_{calc}, (g/m^3)	1.823	1.509	1.207
μ (mm^{-1})	0.432	0.637	0.074
F(000)	3536	436	372
crystal size (mm)	0.14×0.12×0.08	0.15×0.03×0.02	0.15×0.12×0.05
2θ range (°)	1.764–30.753	3.232–27.460	3.518–27.458
index ranges	−32<=h<=23, −20<=k<=21, −23<=l<=20	−12<=h<=12, −13<=k<=13, −14<=l<=14	−14<=h<=14, −8<=k<=8, −15<=l<=17
reflns collected	24691	9687	7850
Indep reflns/R_{int}	7993/0.0480	4232/0.0560	2171/0.0610
parameters	532	235	120
GOF on F^2	1.014	1.006	1.054
R_1, wR_2 [I>2$\sigma(I)$]	0.0482, 0.0917	0.0448, 0.0875	0.0476, 0.1030
R_1, wR_2 (all data)	0.0835, 0.1007	0.0861, 0.1009	0.0740, 0.1143
$\Delta\rho_{min,\ max}$ / e Å^{-3}	0.369, −0.433	0.394, −0.314	0.221, -0.243

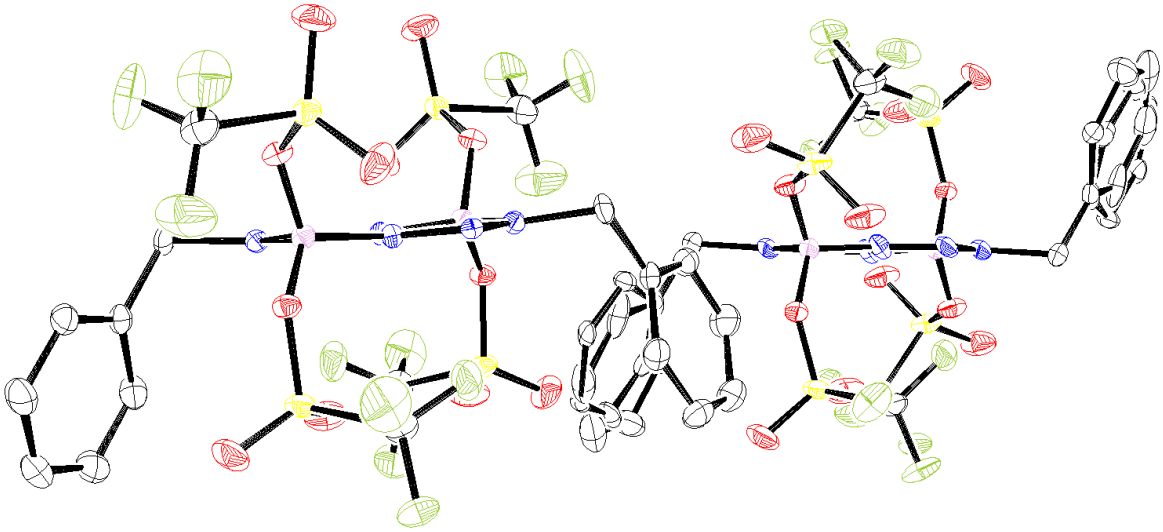

Figure S14. Molecular structure of **2** with two benzyl conformers in the crystal. (Thermal ellipsoids at 50% probability. Hydrogen atoms are omitted for clarity. Two independent molecules are shown.)

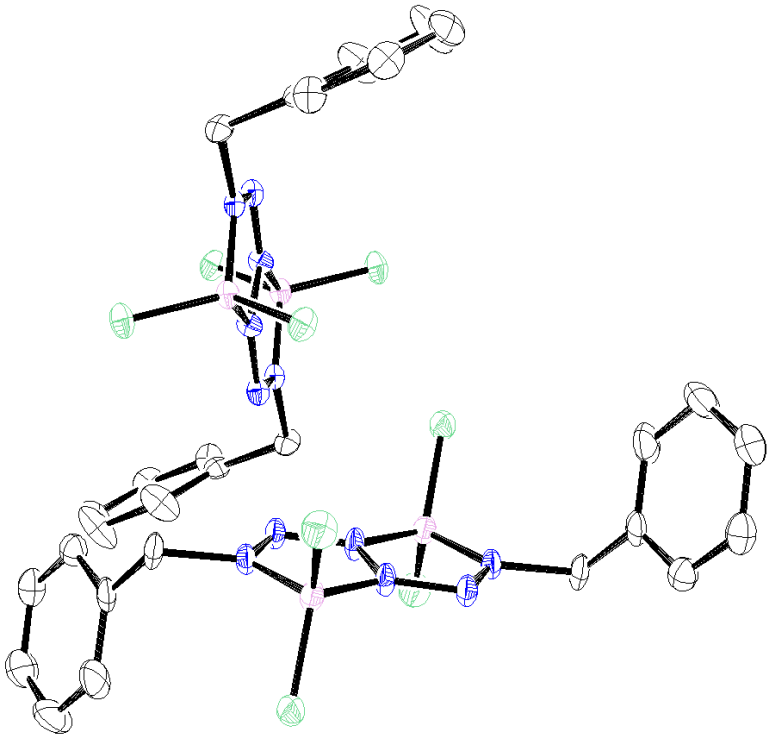

Figure S15. Molecular structure of **3** in the crystal (Thermal ellipsoids at 50% probability. Hydrogen atoms are omitted for clarity. Two independent molecules are shown.)

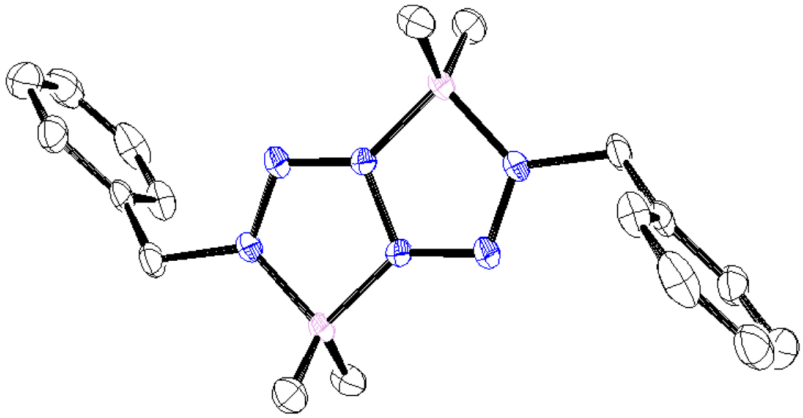

Figure S16. Molecular structure of **4** in the crystal (Thermal ellipsoids at 50% probability. Hydrogen atoms are omitted for clarity.)

3. Absorption Spectra

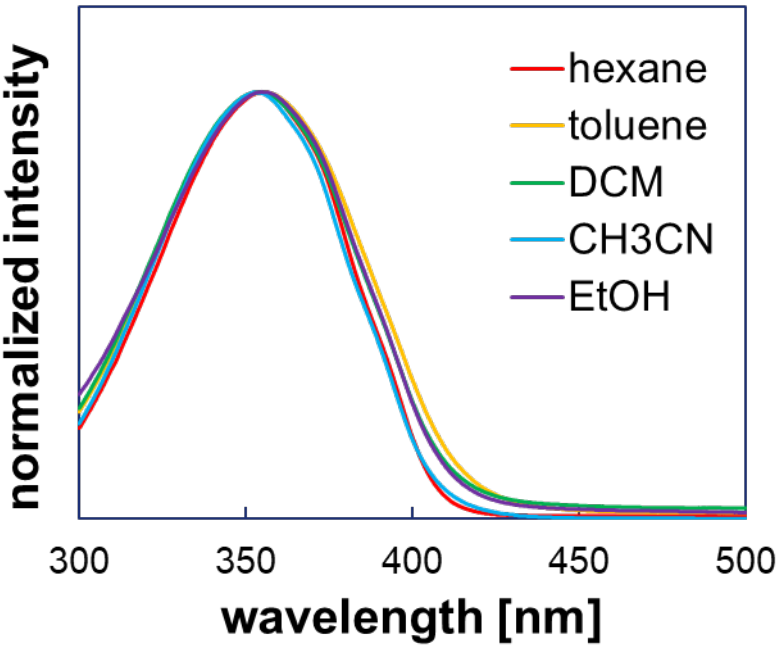

Figure S17. UV–vis absorption spectra of **2** (50.0 μM) at room temperature in hexane, toluene, dichloromethane, acetonitrile, and ethanol.

4. Cyclic Voltammetry

Cyclic voltammetry (CV) of **1** – **4** (2.00 mM each) was carried out in dry dichloromethane under ambient air at room temperature, using $^{n}Bu_4NPF_6$ (0.10 M) as the supporting electrolyte. A glassy carbon disk working electrode, a platinum wire counter electrode, and an Ag/Ag^+ reference electrode were employed with the scan rate of 50 mV s^{-1}. All potentials were referenced to the Cp_2Fe/Cp_2Fe^+ (Fc/Fc^+) redox couple at 0.0 V.

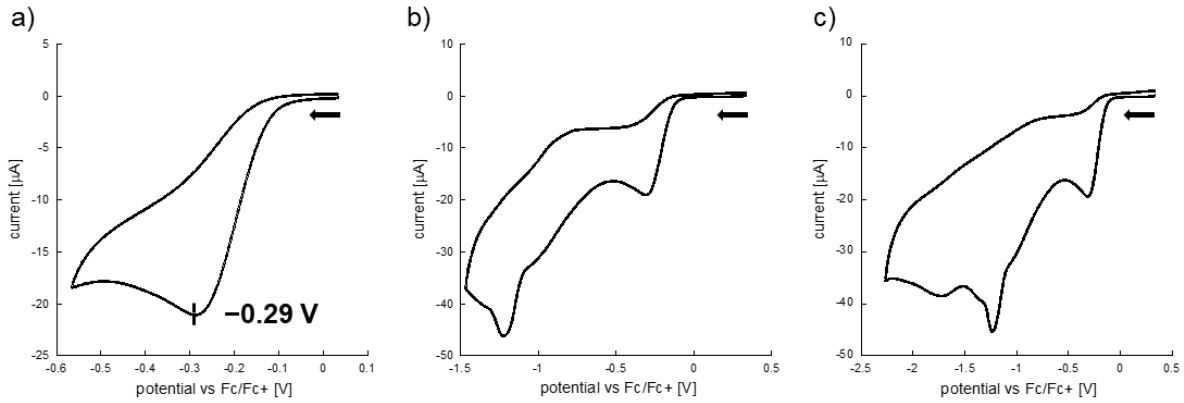

Figure S18. Cyclic voltammograms in the reduction range for a 2.00 mM solution of **2** in CH_2Cl_2.

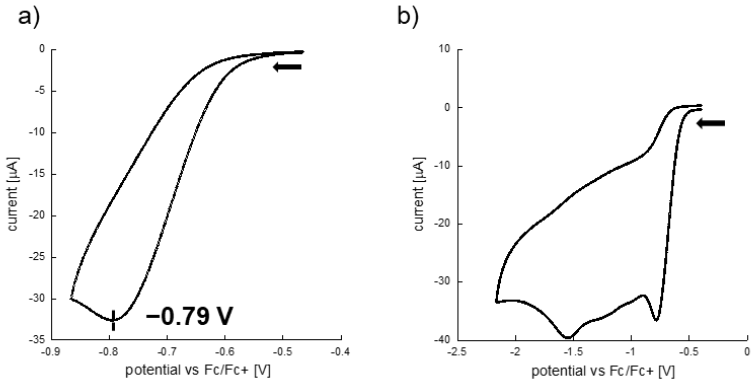

Figure S19. Cyclic voltammograms in the reduction range for a 2.00 mM solution of **3** in CH_2Cl_2.

5. Computational Study

All calculations were performed by using the Gaussian 16 program.[39] The geometry optimization and TD-DFT calculations[40] to estimate UV-vis spectrum of **1**,[33] **2**, **3**, and **4** were performed using the B3LYP[41] functional and the 6-31+G(d) basis set[42] and employing SMD solvation model[43] with dichloromethane as the solvent and empirical dispersion correction (DFT-D3BJ).[44]

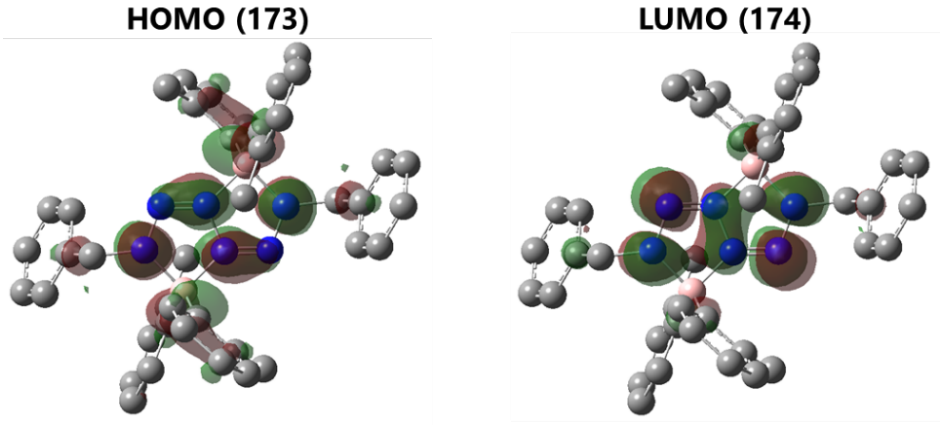

Figure S20. Calculated frontier orbitals of **1** (isovalue = 0.03).

Table S2. Calculated excitation energies and oscillator strengths for **1** at the B3LYP/6-31+G(d) level of theory.

Excited State 1: Singlet-A 3.0119 eV 411.64 nm f=0.3456 <S**2>=0.000
173 -> 174 0.69626
This state for optimization and/or second-order correction.
Total Energy, E(TD-HF/TD-DFT) = -2003.99654823
Copying the excited state density for this state as the 1-particle RhoCI density.

Excited State 2: Singlet-A 3.3249 eV 372.89 nm f=0.0246 <S**2>=0.000
171 -> 174 0.69399

Excited State 3: Singlet-A 3.3308 eV 372.24 nm f=0.0000 <S**2>=0.000
172 -> 174 0.69974

Excited State 4: Singlet-A 3.4187 eV 362.66 nm f=0.0000 <S**2>=0.000
169 -> 174 0.69804

Excited State 5: Singlet-A 3.4291 eV 361.56 nm f=0.0250 <S**2>=0.000
170 -> 174 0.69941

Excited State 6: Singlet-A 3.5768 eV 346.64 nm f=0.0000 <S**2>=0.000
168 -> 174 0.69731

Excited State 7: Singlet-A 3.5851 eV 345.83 nm f=0.0131 <S**2>=0.000
167 -> 174 0.70109

Excited State 8: Singlet-A 3.6548 eV 339.24 nm f=0.0000 <S**2>=0.000
166 -> 174 0.69483

Excited State 9: Singlet-A 3.6689 eV 337.93 nm f=0.0171 <S**2>=0.000
165 -> 174 0.69963

Excited State 10: Singlet-A 3.9388 eV 314.77 nm f=0.0000 <S**2>=0.000
162 -> 174 -0.28737
164 -> 174 0.64142

Excited State 11: Singlet-A 3.9769 eV 311.76 nm f=0.0060 <S**2>=0.000
161 -> 174 -0.25556
163 -> 174 0.65636

Excited State 12: Singlet-A 4.0065 eV 309.46 nm f=0.0000 <S**2>=0.000
162 -> 174 0.64150
164 -> 174 0.29010

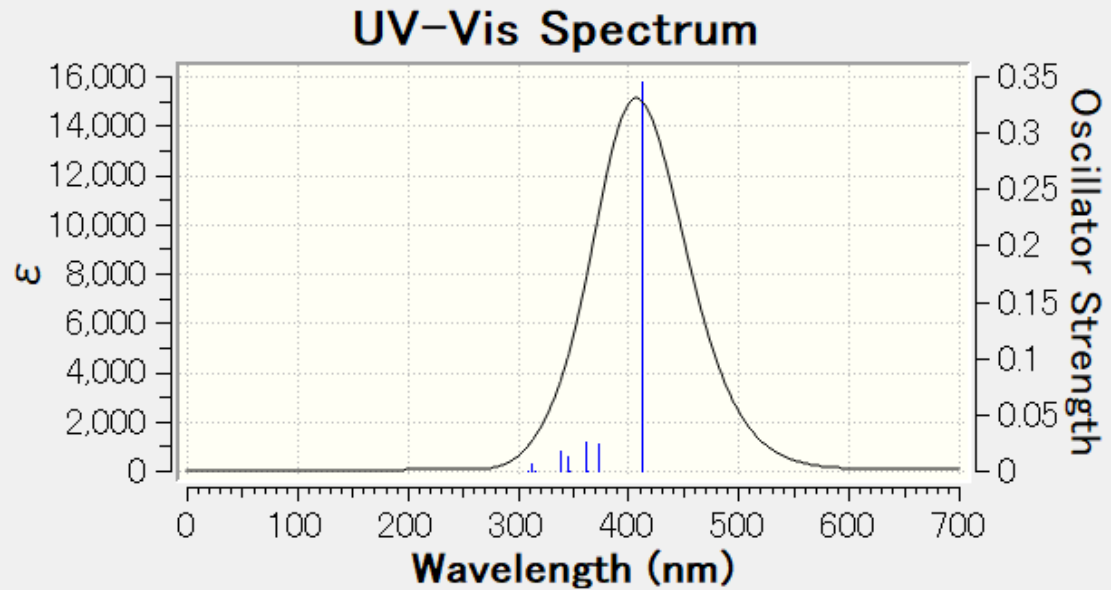

Figure S21. Simulated absorption spectrum (DCM) of **1**.

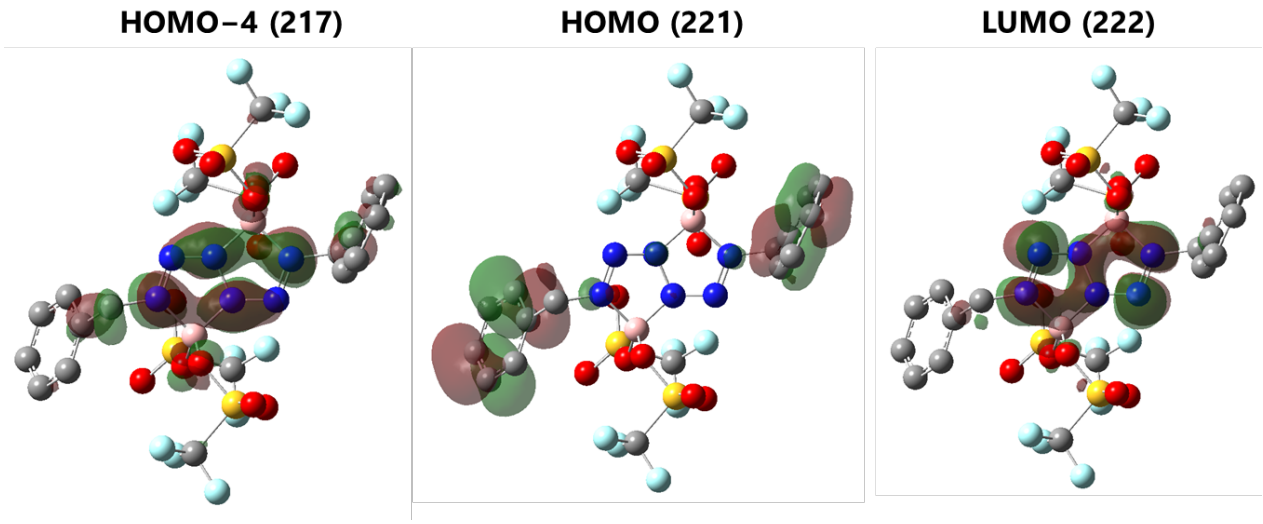

Figure S22. Calculated frontier orbitals of **2** (isovalue = 0.03)

Table S3. Calculated excitation energies and oscillator strengths for **2** at the B3LYP/6-31+G(d) level of theory.

Excited State 1: Singlet-A 2.7604 eV 449.15 nm f=0.1065 <S**2>=0.000
219 -> 222 0.11095
220 -> 222 0.15766
221 -> 222 0.67816
This state for optimization and/or second-order correction.
Total Energy, E(TD-HF/TD-DFT) = -4766.01997516
Copying the excited state density for this state as the 1-particle RhoCI density.

Excited State 2: Singlet-A 2.7963 eV 443.39 nm f=0.0083 <S**2>=0.000
219 -> 222 -0.18026
220 -> 222 0.66972
221 -> 222 -0.12620

Excited State 3: Singlet-A 2.8432 eV 436.07 nm f=0.0026 <S**2>=0.000
219 -> 222 0.67309
220 -> 222 0.15415
221 -> 222 -0.14631

Excited State 4: Singlet-A 2.8764 eV 431.03 nm f=0.0013 <S**2>=0.000
218 -> 222 0.70594

Excited State 5: Singlet-A 3.8436 eV 322.58 nm f=0.4243 <S**2>=0.000
217 -> 222 0.70241

Excited State 6: Singlet-A 4.5574 eV 272.05 nm f=0.0009 <S**2>=0.000

208 -> 222 0.11538
209 -> 222 -0.11120
215 -> 222 0.25244
216 -> 222 0.29537
220 -> 223 0.14074
221 -> 223 0.52438

Excited State 7: Singlet-A 4.5781 eV 270.82 nm f=0.0051 <S**2>=0.000
208 -> 222 0.14368
209 -> 222 -0.14922
215 -> 222 0.39550
216 -> 222 0.18549
220 -> 223 -0.36118
221 -> 223 -0.31091

Excited State 8: Singlet-A 4.5973 eV 269.69 nm f=0.0211 <S**2>=0.000
215 -> 222 0.16198
216 -> 222 0.10009
219 -> 223 -0.14903
220 -> 223 0.56758
221 -> 223 -0.31410

Excited State 9: Singlet-A 4.6542 eV 266.39 nm f=0.0040 <S**2>=0.000
219 -> 223 0.68180
220 -> 223 0.13467
221 -> 223 -0.10336

Excited State 10: Singlet-A 4.6855 eV 264.61 nm f=0.0008 <S**2>=0.000
218 -> 223 0.70333

Excited State 11: Singlet-A 4.8960 eV 253.24 nm f=0.0026 <S**2>=0.000
215 -> 222 -0.37125
216 -> 222 0.54097
217 -> 223 0.16604
221 -> 223 -0.10978

Excited State 12: Singlet-A 4.9692 eV 249.51 nm f=0.0026 <S**2>=0.000
214 -> 222 0.67796
216 -> 222 -0.13811

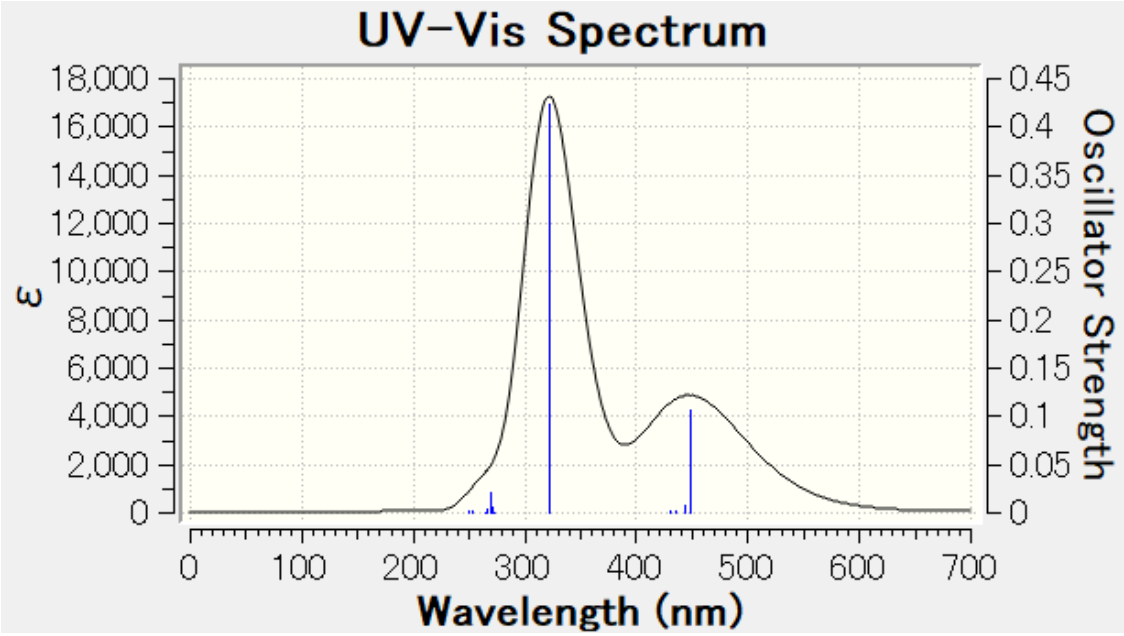

Figure S23. Simulated absorption spectrum (DCM) of **2**.

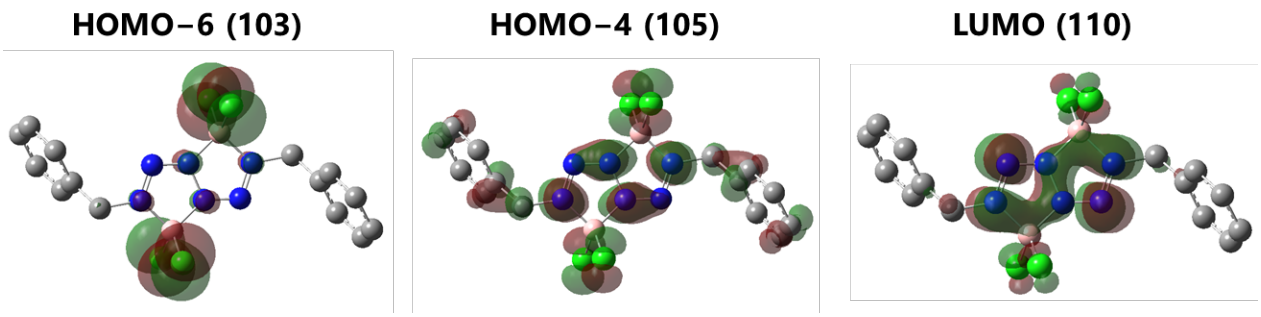

Figure S24. Calculated frontier orbitals of **3** (isovalue = 0.03)

Table S4. Calculated excitation energies and oscillator strengths for **3** at the B3LYP/6-31+G(d) level of theory.

Excited State 1: Singlet-AU 3.0206 eV 410.47 nm f=0.0377 <S**2>=0.000
105 ->110 -0.11155
107 ->110 -0.14850
109 ->110 0.67982
This state for optimization and/or second-order correction.
Total Energy, E(TD-HF/TD-DFT) = -2761.04289622
Copying the excited state density for this state as the 1-particle RhoCI density.

Excited State 2: Singlet-AG 3.0239 eV 410.02 nm f=0.0000 <S**2>=0.000
106 ->110 -0.14633
108 ->110 0.68899

Excited State 3: Singlet-AU 3.1125 eV 398.34 nm f=0.0072 <S**2>=0.000
107 ->110 0.68912
109 ->110 0.15076

Excited State 4: Singlet-AG 3.1185 eV 397.58 nm f=0.0000 <S**2>=0.000
106 ->110 0.69004
108 ->110 0.14708

Excited State 5: Singlet-AU 3.4440 eV 360.00 nm f=0.3870 <S**2>=0.000
105 ->110 0.69270
109 ->110 0.10979

Excited State 6: Singlet-AG 4.0697 eV 304.65 nm f=0.0000 <S**2>=0.000
104 ->110 0.70290

Excited State 7: Singlet-AU 4.1767 eV 296.85 nm f=0.0654 <S**2>=0.000
103 ->110 0.70240

Excited State 8: Singlet-AU 4.2704 eV 290.33 nm f=0.0002 <S**2>=0.000
101 ->110 0.69049

Excited State 9: Singlet-AG 4.3116 eV 287.56 nm f=0.0000 <S**2>=0.000
102 ->110 0.69548

Excited State 10: Singlet-AU 4.4991 eV 275.58 nm f=0.0189 <S**2>=0.000
100 ->110 0.69838

Excited State 11: Singlet-AG 4.5388 eV 273.17 nm f=0.0000 <S**2>=0.000
99 ->110 0.70037

Excited State 12: Singlet-AU 4.7863 eV 259.04 nm f=0.0105 <S**2>=0.000
98 ->110 0.70068

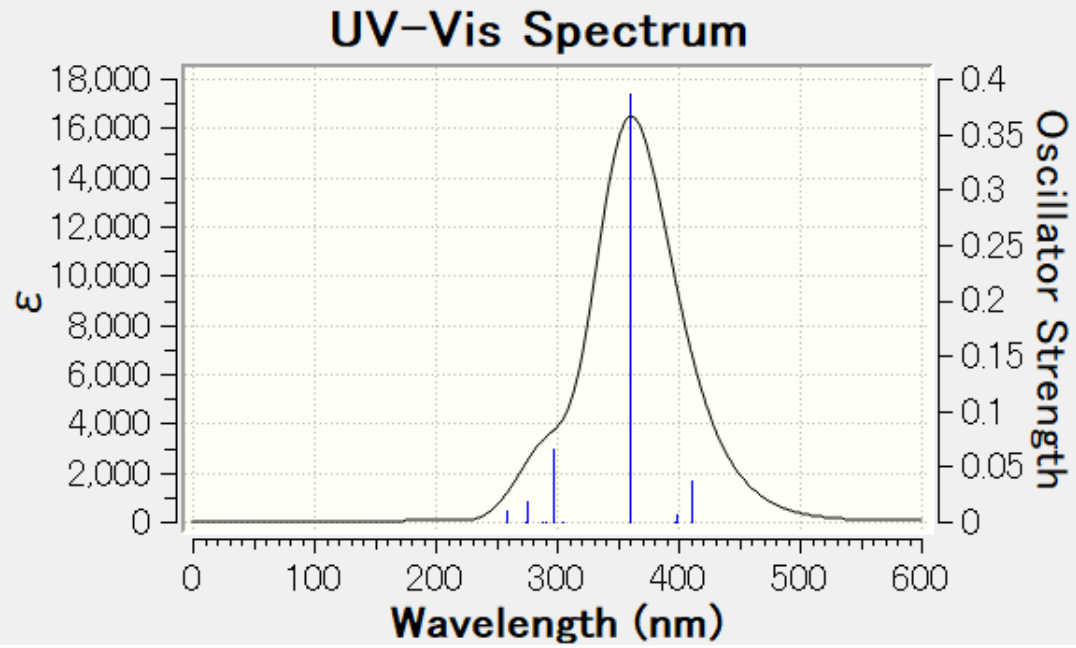

Figure S25. Simulated absorption spectrum (DCM) of **3**.

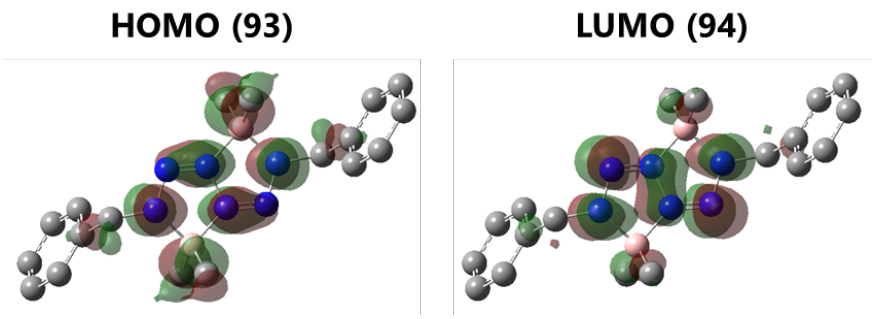

Figure S26. Calculated frontier orbitals of **4** (isovalue = 0.03)

Table S5. Calculated excitation energies and oscillator strengths for **4** at the B3LYP/6-31+G(d) level of theory.

Excited State 1: Singlet-AU 3.1220 eV 397.13 nm f=0.5223 <S**2>=0.000
93 -> 94 0.70563
This state for optimization and/or second-order correction.
Total Energy, E(TD-HF/TD-DFT) = -1079.75436316
Copying the excited state density for this state as the 1-particle RhoCI density.

Excited State 2: Singlet-AG 4.1849 eV 296.27 nm f=0.0000 <S**2>=0.000
92 -> 94 0.69909

Excited State 3: Singlet-AU 4.2341 eV 292.82 nm f=0.0168 <S**2>=0.000
91 -> 94 0.70209

Excited State 4: Singlet-AG 4.3540 eV 284.76 nm f=0.0000 <S**2>=0.000
87 -> 94 0.10210
90 -> 94 -0.15090
93 -> 95 0.67190

Excited State 5: Singlet-AG 4.3873 eV 282.60 nm f=0.0000 <S**2>=0.000
90 -> 94 0.68810
93 -> 95 0.14745

Excited State 6: Singlet-AU 4.3893 eV 282.47 nm f=0.0019 <S**2>=0.000
89 -> 94 0.70337

Excited State 7: Singlet-AU 4.5378 eV 273.22 nm f=0.0040 <S**2>=0.000
93 -> 96 0.70319

Excited State 8: Singlet-AG 4.5810 eV 270.65 nm f=0.0000 <S**2>=0.000
93 -> 97 0.69354

Excited State 9: Singlet-AU 4.7153 eV 262.94 nm f=0.0027 <S**2>=0.000
93 -> 98 0.70183

Excited State 10: Singlet-AG 4.8283 eV 256.79 nm f=0.0000 <S**2>=0.000
87 -> 94 0.15108
93 -> 97 -0.10264
93 -> 99 0.66613

Excited State 11: Singlet-AG 5.0072 eV 247.61 nm f=0.0000 <S**2>=0.000
88 -> 94 0.11167
93 ->100 0.67823

Excited State 12: Singlet-AU 5.0733 eV 244.39 nm f=0.0006 <S**2>=0.000
86 -> 94 0.69212

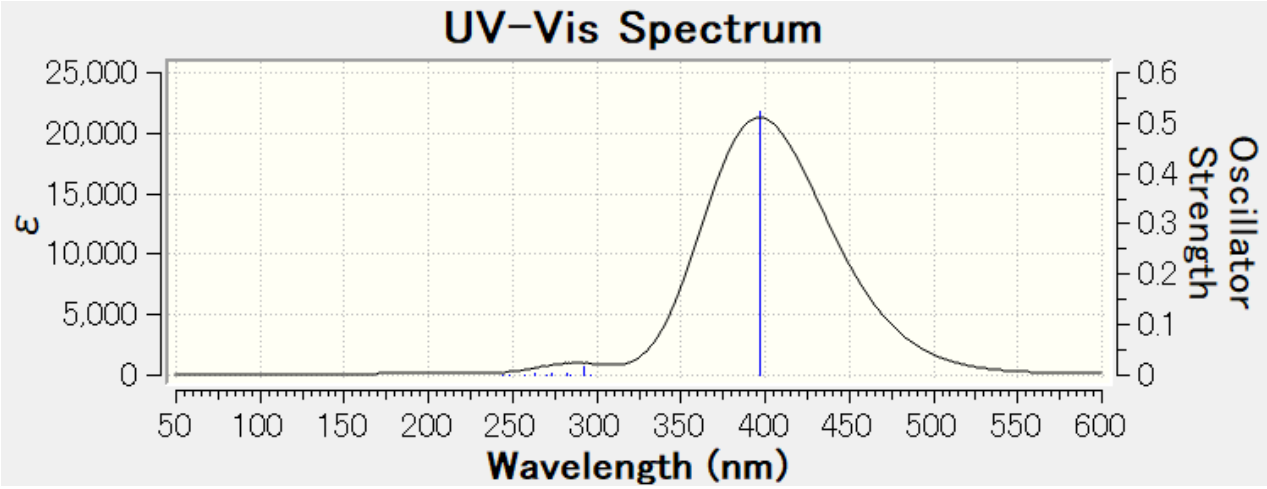

Figure S27. Simulated absorption spectrum (DCM) of **4**.

6. Study for the Stability of Compounds

Solutions of **2**, **3**, and **4** in $CDCl_3$ were left under air at room temperature for three days, and no change of ^1H NMR spectra was observed for any of the compounds. A drop of deionized water was added to solutions of **2**, **3**, and **4** in $CDCl_3$, and the mixtures were rigorously stirred at room temperature under air. After stirring for 8 h, the ^1H NMR spectra of **3** and **4** showed no changes, whereas the solution of **2** exhibited new signals in the 5.2–5.5 ppm region, suggesting partial decomposition (**Figure S28**).

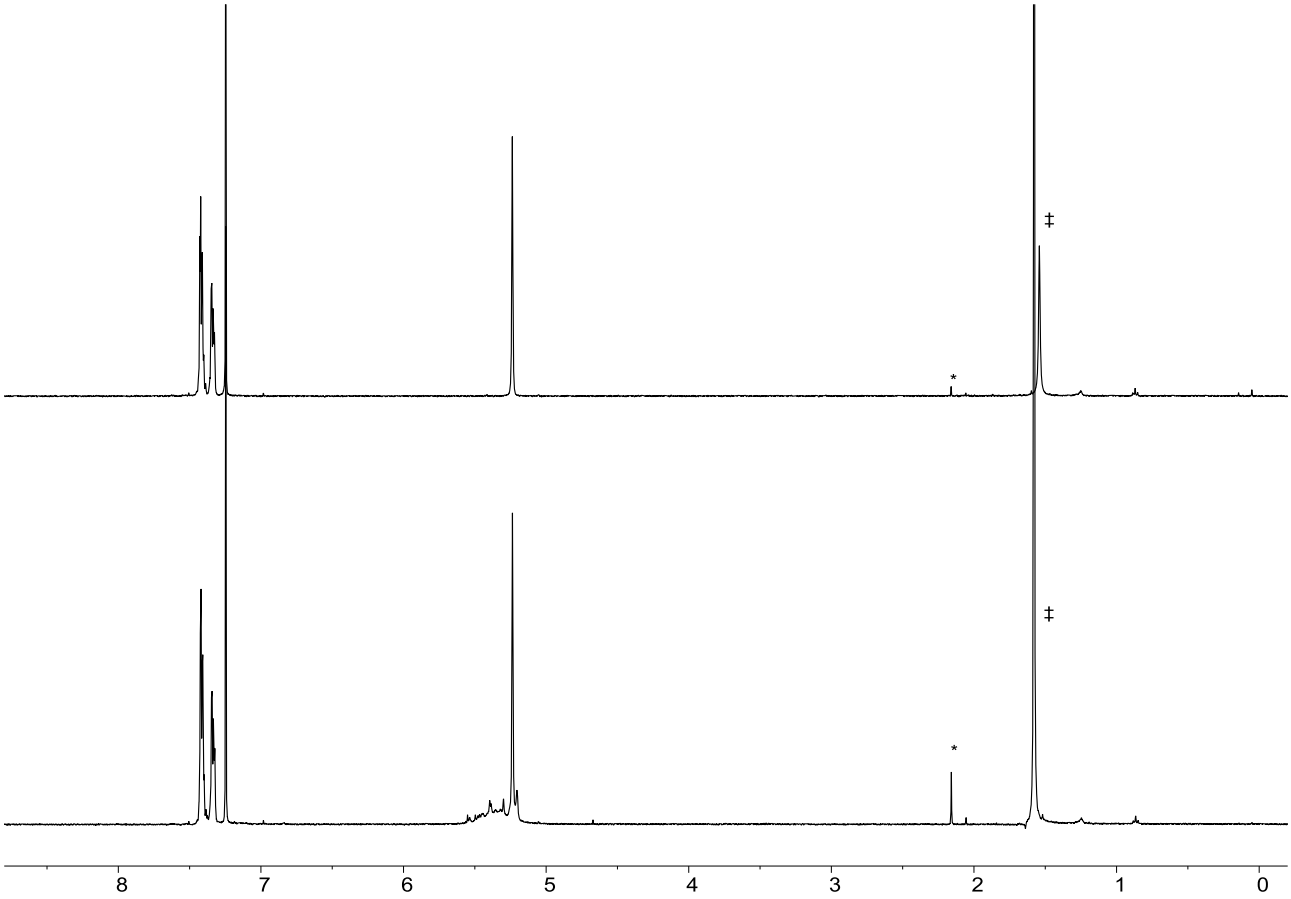

Figure S28. ^1H NMR spectrum of **2** in $CDCl_3$ and after 8 h at RT in the presence of H_2O (*: acetone, ‡: H_2O).

7. References

35 CrysAlisPRO, Oxford Diffraction/Agilent Technologies UK Ltd, Yarnton, England, (2015).

36 O. V. Dolomanov, Bourhis, L. J., Gildea, R. J., Howard, J. A. K. & Puschmann, H., *J. Appl. Crysy*., 2009, **42**, 339–341.

37 C. A. Kabuto, S.; Kwon, E., *J. Cryst. Soc. Jpn.,* 2009, **51**, 218–224.

38 G. Sheldrick, *Act. Cryst. Sec. C,* 2015, **71**, 3–8.

39 M. J. Frisch, G. W. Trucks, H. B. Schlegel, G. E. Scuseria, M. A. Robb, J. R. Cheeseman, G. Scalmani, V. Barone, G. A. Petersson, H. Nakatsuji, X. Li, M. Caricato, A. V. Marenich, J. Bloino, B. G. Janesko, R. Gomperts, B. Mennucci, H. P. Hratchian, J. V. Ortiz, A. F. Izmaylov, J. L. Sonnenberg, Williams, F. Ding, F. Lipparini, F. Egidi, J. Goings, B. Peng, A. Petrone, T. Henderson, D. Ranasinghe, V. G. Zakrzewski, J. Gao, N. Rega, G. Zheng, W. Liang, M. Hada, M. Ehara, K. Toyota, R. Fukuda, J. Hasegawa, M. Ishida, T. Nakajima, Y. Honda, O. Kitao, H. Nakai, T. Vreven, K. Throssell, J. A. Montgomery Jr., J. E. Peralta, F. Ogliaro, M. J. Bearpark, J. J. Heyd, E. N. Brothers, K. N. Kudin, V. N. Staroverov, T. A. Keith, R. Kobayashi, J. Normand, K. Raghavachari, A. P. Rendell, J. C. Burant, S. S. Iyengar, J. Tomasi, M. Cossi, J. M. Millam, M. Klene, C. Adamo, R. Cammi, J. W. Ochterski, R. L. Martin, K. Morokuma, O. Farkas, J. B. Foresman, D. J. Fox, Gaussian 16, Revision C.01, ver. Wallingford, CT, 2016.

40 (a) C. Adamo, D. Jacquemin, *Chem. Soc. Rev.,* 2013, **42**, 845–856; (b) A. D. Laurent, C. Adamo, D. Jacquemin, *Phys. Chem. Chem. Phys*., 2014, **16**, 14334–14356.

41 (a) C. Lee, W. Yang, R. G. Parr, *Phys. Rev. B,* 1988, **37**, 785–789; (b) A. D. Becke, *Phys. Rev. A,* 1988, **38**, 3098–3100; (c) B. Miehlich, A. Savin, H. Stoll, H. Preuss, *Chem. Phys. Lett.,* 1989, **157**, 200–206.

42 S. Huzinaga, J. Andzelm, M. Klobukowski, E. Radzio-Andzelm, Y. Sakai, H. Tatewaki, Gaussian basis sets for molecular calculations, Elsevier, 1984.

43 A. V. Marenich, C. J. Cramer, D. G. Truhlar, *J. Phys. Chem. B* 2009, **113**, 6378–6396.

44 (a) S. Grimme, J. Antony, S. Ehrlich, H. Krieg, *J. Chem. Phys*., 2010, **132**, 154104.; (b) S. Grimme, S. Ehrlich, L. Goerigk, *J. Comput. Chem*., 2011, **32**, 1456-1465.